JAMA Facial Plastic Surgery | Original Investigation

Biomechanic Factors Associated With Orbital Floor Fractures

Sagar Patel, MD; Christopher Andrecovich, MS; Michael Silverman, BS; Liying Zhang, PhD; Mahdii Shkoukani, MD

IMPORTANCE Orbital floor fractures are commonly seen in clinical practice, yet the etiology underlying the mechanism of fracture is not well understood. Current research focuses on the buckling theory and hydraulic theory, which implicate trauma to the orbital rim and the globe, respectively.

OBJECTIVE To elucidate and define the biomechanical factors involved in an orbital floor fracture.

DESIGN, SETTING, AND PARTICIPANTS A total of 10 orbits from 5 heads (3 male and 2 female) were used for this study. These came from fresh, unfixed human postmortem cadavers that were each selected so that the cause of death did not interfere with the integrity of orbital walls. Using a drop tower with an accelerometer, we measured impact force on the globe and rim of cadaver heads affixed with strain gauges.

RESULTS The mean impacts for rim and globe trauma were 3.9 J (95% CI, 3.4-4.3 J) and 3.9 J (95% CI, 3.5-4.3 J), respectively. Despite similar impact forces to the globe and rim, strain-gauge data displayed greater mean strain for globe impact (6563 μS) compared with rim impact (3530 μS); however, these data were not statistically significant (95% CI, 3598-8953 μS; $P = .94$).

CONCLUSIONS AND RELEVANCE Our results suggest that trauma directly to the globe predisposes a patient to a more posterior fracture while trauma to the rim demonstrates an anterior predilection. Both the hydraulic and buckling mechanisms of fracture exist and demonstrate similar fracture thresholds.

LEVEL OF EVIDENCE NA.

JAMA Facial Plast Surg. doi:10.1001/jamafacial.2016.2153
Published online March 9, 2017.

Author Affiliations: Department of Otolaryngology, Wayne State University, Detroit, Michigan (Patel, Silverman, Shkoukani); Department of Biomedical Engineering, Wayne State University, Detroit, Michigan (Andrecovich, Zhang).

Corresponding Author: Sagar Patel, MD, Facial Plastic Surgery Associates, 6655 Travis St, Ste 900, Houston, TX 77030 (spatel@todaysface.com).

Blowout fractures of the orbit, a term first put forth by Smith and Regan,[1] describes a specific set of fractures of the orbital bone often resulting from blunt trauma. Most commonly this refers to fractures of the orbital floor but can also include the medial orbital wall or the roof of the orbit. To further explain the mechanism underlying this type of fracture, the "buckling" theory and the "hydraulic" theory have been previously proposed.[2,3] The buckling theory contends that injury—but not fracture—to the infraorbital rim then leads to a fracture of the more delicate orbital floor. The hydraulic theory purports that insult to the globe itself transmits pressure to the orbital floor, thereby inducing a fracture.[4] However, in attempting to evaluate these theories, many previous studies have had inconsistences in their study design. For example, several studies[5,6] used fixed cadaveric skulls and failed to properly quantify the forces applied.

Recent work by Ahmad et al[7] analyzed direct trauma to both the globe and rim in the orbits of fresh, intact, human postmortem cadavers using strain gauges in an attempt to test both the hydraulic and buckling mechanisms. Their experimental setup allowed for both qualitative and quantitative assessment of orbital floor fracture and demonstrated that the buckling mechanism tends to produce fractures in the anterior and anteromedial aspects of the orbital floor, whereas the hydraulic mechanism tends to produce fractures in the posterior aspects of the orbital floor. Our hypothesis is that both the hydraulic and buckling theories will manifest similar force thresholds required for fracture; however, anatomical fracture patterns will differ and can provide clinical data on the necessity of ophthalmologic evaluation.

Methods

The study was exempt from institutional review board approval because there were no HIPAA issues or human studies and only cadavers were used. A total of 10 orbits from 5 heads (3 male and 2 female) were used for this study. These came from

fresh, unfixed human postmortem cadavers that were each selected so that the cause of death did not interfere with the integrity of orbital walls. The experiments were conducted at 61 to 168 days postmortem. Frozen cadaver heads were allowed to reach room temperature to simulate normal conditions of orbital floor trauma. A standard 24-hour thaw cycle was used for all heads. A sublabial incision was performed to expose anterior maxillary wall. Next, a Caldwell-Luc approach was performed by using an osteotome. A 1.5-cm antrostomy was created on the anterior face of the maxillary sinus. The sinus mucosal lining was meticulously removed using a periosteal elevator. Care was taken to avoid creating artifactual fractures of the orbital floor. The antral roof was cleaned with acetone on a cotton bud, and a single-foil uniaxial strain gauge was fixed to the cleansed surface. Consistent gauge placement was achieved by placing the gauge at the medial border of the infraorbital canal and 5 mm posterior to the inferior orbital rim. A MotionXtra HG-100K camera (Redlake) was used to collect high-speed video of the impacts at a rate of 1000 frames per second. The strain-gauge data were collected at a rate of 20 000 Hz using a TDAS Pro (Diversified Technologies). After the dissection and placement of the strain gauges, each cadaver head was scanned with computed tomography (CT) to ensure no fractures had been created.

Because intraocular pressure is known to fall rapidly after death, it was necessary to reinflate the globes to within the normal range to reproduce in vivo conditions. Between 0.4 and 1.2 mL of a solution normal saline, injected into both the anterior and the posterior chambers of the globe, was found to maintain intraocular pressure at normotensive levels (10-20 mm Hg) for about 15 minutes. Intraocular pressure was measured using a tonometer. The right orbit of each cadaver was used to study the hydraulic mechanism with the focal impact being directed onto the reinflated right globe. The left orbit was used to study the buckling mechanism with the impact being directed onto the midpoint of the infraorbital rim.

The impactor used was a cylindrical mass weighing 397 g with beveled edges that minimized any soft-tissue injury following impact. The weight was released through a larger cylindrical tube from a measured height of 1.74 m. Initially the drop height needed to achieve impact of 4.0 J was obtained using the potential energy formula: $PE = m \times g \times h$. In the initial test, the actual impactor velocity data were obtained from video tracking and compared with the calculation of the velocity just before impact by

$$v = \sqrt{2gh}.$$

We found that our actual impacts produced about half the desired energy when the impactor was dropped from this height. To help determine the energy levels necessary required to produce orbit fracture, finite element (FE) analysis of orbital fracture from various impact energies was carried out using a human head FE model with detailed ocular anatomy.[8,9] The globe model included the cornea, sclera, aqueous humor, iris, lens, zonules, ciliary body, retina, and vitreous humor. The extraocular structures included 6 muscles, optic nerve, fat, and the orbit. The FE model was validated against experimental measurements from cadaveric facial impact tests and globe impact tests from different projectile types and velocities. The simulated impact energies of 2.0, 3.0, 5.0, and 10.0 J were consistent with the orbit fracture impact energy used in the orbital fracture experiments reported by Rhee et al.[10]

Using video tracking and the accelerometer measurements, we determined a desired height where we consistently obtained 4.0-J impacts. An accelerometer was used in each experiment to measure the actual velocity of the mass at the impact of the rim or globe.

Following an impact, the circuitry was checked for electrical integrity, and the orbital floor was inspected for fractures transantrally using a powerful light source. In addition, the floor was carefully explored with a periosteal elevator to palpate any fractures. After all heads were tested, each received a CT maxillofacial with 0.625-mm cuts of the orbit using a VCT 64-slice CT scanner system. Next, a probe was used to identify gross fractures. These fractures were identified using a permanent marker, and, using a macrolens and a Canon EOS Rebel T3i DSLR camera, the fracture patterns were documented. Finally, using a fine-caliper, measurements were taken at 7 locations on the orbital floor as depicted in **Figure 1**. To ob-

Key Points

Question Does the anatomical pattern of an orbital floor fracture delineate the etiologic biomechanical force applied and provide further clinical data?

Findings In this cadaver study, despite similar impact forces to the globe and rim, strain-gauge data displayed greater mean strain for globe impact, suggesting that trauma directly to the globe predisposes a patient to a more posterior fracture, whereas trauma to the rim demonstrates an anterior predilection. Both the hydraulic and buckling mechanisms of fracture exist and demonstrate similar fracture thresholds.

Meaning The anatomical fracture pattern can determine the likelihood of globe impact. This will help a physician determine the importance and urgency of an ophthalmologic evaluation.

Figure 1. Fracture Thickness Map

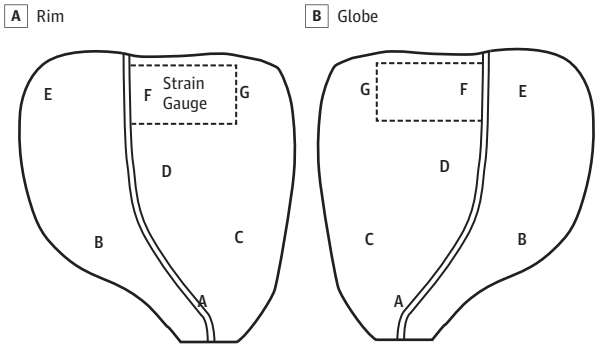

Fracture map showing regions from where bone thickness measurements were taken (A-G) and approximate position of strain gauge (dashed boxes). The central solid double line demonstrates the approximate location of infraorbital nerve as it courses through the orbital floor.

Figure 2. Fracture Map

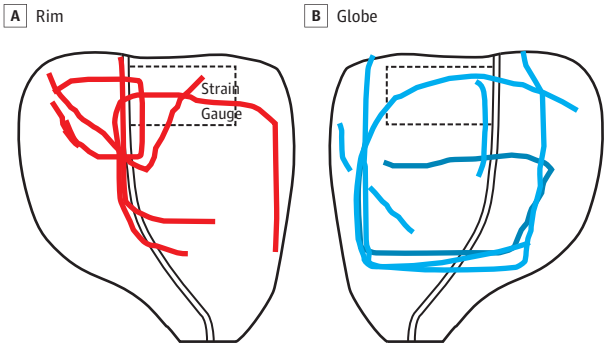

A, Rim; 3.86 J; maximum strain 5419 microstrains (μS); minimum strain, −6906 μS; maximum shear, 5395 Pa. B, Globe, 3.88 J; maximum strain, 6275 μS; minimum strain, −6043 μS; maximum shear, 6085 Pa.

Figure 3. Orbital Floor Thickness Map

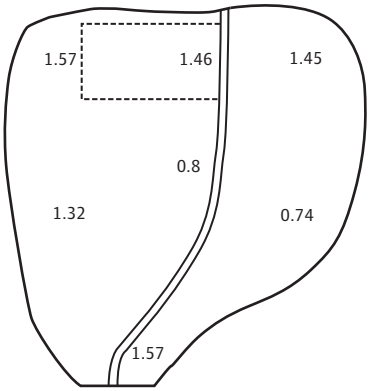

Values of defined regions listed in millimeters. The approximate position of strain gauge (dashed box) is displayed. The central solid double line demonstrates the approximate location of infraorbital nerve as it courses through the orbital floor.

tain the most accurate measurements of each location, the bone was removed using a Rongeur from anterior to posterior.

Data were analyzed using standard statistical measures. For the fracture pattern analysis, an injury severity scale was developed. Based on the range of fracture size, 2 levels of severity were developed: mild and severe. The length of each fracture was measured by approximating the shape and size on a 2-dimensional image of the orbital floor. A measurement of the anteroposterior length of the orbital floor was determined. Using ImageJ software, this measurement was used to develop a scaling factor. Once a scaling factor was determined for each specimen, the fractures could be traced in the software to determine their lengths in millimeters. Based on the results of these measurements, it was determined that fractures from an impact that totaled less than 15 mm would be considered mild, whereas fractures that were 15 mm or greater would be considered severe. Separating the resultant fractures yielded 2 mild fractures and 7 severe fractures. One impact resulted in a nonfracture scenario and was not considered in this analysis.

Results

A total of 5 human postmortem cadaver heads were tested. The mean (SD) age of the heads was 59.4 (8.0) years. The mean body mass index, calculated as weight in kilograms divided by height in meters squared, was 26.6 (7.6). Three male and 2 female heads were used. A radiological assessment revealed fractures in 3 of the 10 orbits, whereas a gross assessment revealed fractures in 9 of the 10 orbits.

A review of the fracture patterns revealed that overall, the rim trauma produces smaller more anterior fractures, whereas the globe trauma produces larger and more posterior trauma (**Figure 2**). The mean impacts for rim and globe trauma were 3.9 J (95% CI, 3.4-4.3 J) and 3.9 J (95% CI, 3.5-4.3 J), respectively. Strain-gauge data showed a higher mean strain for globe impact (6563 μS) compared with rim impact (3530 μS); however, these data were not statistically significant (P = .94; 95% CI, 3598-8953 μS).

The mean thicknesses of the orbital floors revealed an overall thickness that was greatest anteriorly. Anterior floor thickness was significantly greater than posterior floor thickness (mean [SD], 1.50 mm [0.50 mm] vs 1.18 mm [0.56 mm]; P = .02). It was also noted the bone was thinner medially than laterally. These data were not statistically significant (P = .07). The thickness of the floor decreased going posteriorly toward the apex and then when close to the apex the thickness increased (**Figure 3**).

To determine if the mild fractures were statistically different from the severe fractures, a simple t test was performed using unmatched analysis with 2 tails (P = .03). The mean impact energy of the group of mild fractures was 3.67 J (95% CI, 3.34-3.99), whereas the mean (SD) impact energy of the severe fracture group was 4.0 (0.5) J. A t test comparing these energies resulted in a P value of .49, indicating that the impact energies did not differ significantly.

Maximum principal strain was calculated from measurements of the 3 rosette gauge elements. The maximum principal strains were plotted against the severity of the fractures; mild fractures were represented by a 1 and severe fractures were represented by a 2. A linear regression analysis was performed resulting in the coefficient of determination R^2 value of 0.70 (**Figure 4**). This R^2 value indicates that the magnitude of the strain on the orbital floor influences the severity of the fracture outcome.

With similar energies being imparted to both the globe and rim, evaluations of orbital floor thickness were taken for both the left and right orbits of each specimen. Bilateral symmetry was assumed, and a mean thickness was determined for each specimen. This thickness measurement was evaluated against injury severity, but produced no strong correlation (R^2 = 0.17) (**Figure 5**).

Discussion

Debate regarding the biomechanics of the orbital floor fracture has often juxtaposed the hydraulic theory vs the buck-

Figure 4. Correlation of Strain and Injury Severity

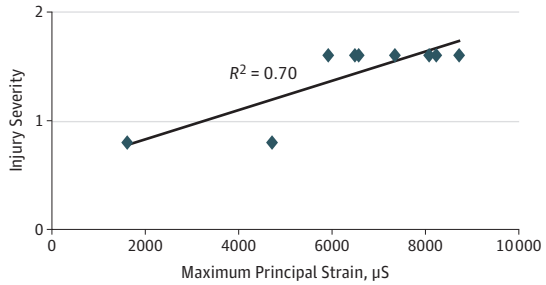

Each data point represents an orbital floor fracture. μS indicates microstrains.

Figure 5. Correlation of Floor Thickness and Injury Severity

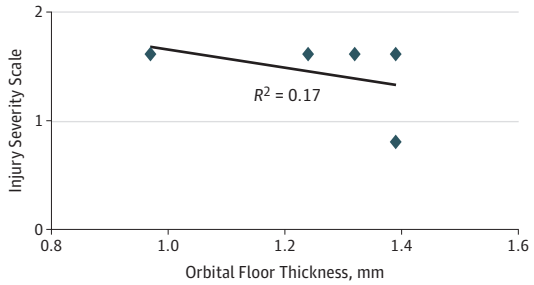

Each data point represents an orbital floor fracture.

ling mechanism. Multiple studies have attempted to compare and contrast one theory vs the other using a plethora of research designs.[5,6] Our initial hypothesis was that both the force transduced posteriorly via the orbital rim (buckling mechanism) and the strain imparted by the globe onto the floor (hydraulic theory) can produce fractures to the orbital floor. It was our belief that the inferior orbital rim, which is a principal horizontal buttress of the facial skeleton, protects the orbital floor and secondary to a cushion effect would produce an anterior fracture in comparison to trauma directly to the globe.

The facial skeleton was previously described to be supported by a system of horizontal beams and vertical buttresses.[11] While the overall anatomy and support of the skeleton requires balanced support from the entire system, the orbital support is due to the horizontal beams of the inferior orbital rim and frontal bar. The frontal bar is the strongest beam,[12] and hence trauma to this zone rarely causes fracture, especially in comparison to the inferior orbital rim.

To establish impact parameters, we used a review of the literature on experimental studies and FE simulation using a validated human head model with detailed orbit and globe anatomy. Previous studies demonstrated a large range of fracture threshold ranging from 2.0 J to 10.8 J. Our FE modeling showed that with 3.0 to 5.0 J impact energy, the maximum principal strain predicted in the floor and medial wall exceeded the fracture limit (0.4% failure strain). Furthermore, model parametric studies on the effect of the bone thickness on resulting maximum principal strain in the orbit suggested that less impact energy would be needed to fracture a thinner orbit bone than a thicker orbit bone. We used a database of CT scan measurements from 87 orbital floors to establish the mean orbital floor thickness. These data were extrapolated from a concurrent study that analyzes the anatomical predictors of orbital floor fracture based on CT scans. A mean thickness of 2 mm was used to perform the modeling. In our cadaveric study, the thickest mean portion of the floor was 1.57 mm. This confirms that our model provided an accurate assessment of the orbit. The FE analysis led us to believe that at about 4.0 J almost all orbital floors should fracture. We were able to reproduce a force of about 3.9 J. Our initial testing using a drop tower, however, did demonstrate that impacts that were intended to be 4.0 J were actually causing only a 1.6-J impact as measured by an accelerometer and video tracking software. The energy loss was largely due to the frictional force between the impactor and the inner surface of the tube. Noting this, adjustments were made and forces, such as friction, were accounted for to reach desired impact severity. Most previous studies did not use an accelerometer to record the actual velocity; therefore, the force of impact, likely based on theoretical calculations, and could possibly be underestimated.

Overall, fracture patterns demonstrated a conceptual difference between the rim and direct globe trauma. The previous study by Ahmad et al[7] notes a similar finding. The injury severity scale did demonstrate a correlation with strain and injury severity. It did not, however, reveal any correlation between severity and thickness of the bone. The inferior orbital rim likely provides a protective cushion in trauma that has direct impacts on the thicker bone of the rim. It was noted that the mean thickness of the orbital bone decreases as one goes posterior and medially on the orbital floor. The concept of the hydraulic theory therefore elicits trauma more toward the center of the floor than the rim. While not statistically significant, our data did show a higher maximum strain of the orbital floor for globe trauma than direct rim trauma. These data imply that on fractures that combine the rim and globe, impact force was probably high and while the orbital floor is repaired to prevent diplopia, the rim should be repaired to reestablish the support of the horizontal beam of the orbital rim. In addition, clinically, when one notes a more posterior fracture it can imply that there was more trauma applied to the globe, and a thorough ophthalmological workup should precede surgery. Finally, it is noteworthy that trauma to the rim produced a fracture pattern more closely abutting the inferior orbital foramen. The area adjacent to the foramen is often weaker as the bone thins prior to splaying to make way for the nerve. While the overall fracture pattern did closely abut the nerve, the foramen also provided a bony casing to prevent nerve transection in the case of an orbital floor fracture.

We also used computed tomographic scans of the heads to confirm and evaluate the presence of fracture. It was noted that while 9 of the orbits showed large nondisplaced fractures after exenteration of the globe, the CT scans did not pick up the fractures in most cases. A plausible explanation for this is that the bonding agent used to attach the strain gauge could have prevented the orbital floor from blowing out. Regardless, a clinical

conclusion is that even if a CT scan does not demonstrate a fracture, if mechanism of trauma is suspected to provide a sufficient force to create a fracture an ophthalmologic evaluation should be pursued.

Limitations

The inherent weakness of our study is the limited sample size. In addition, although our cadavers were not fixed in formalin, they had previously been frozen and were not fresh cadavers.

Conclusions

To our knowledge, our study was the first to use a combination of strain gauges, high-speed video recording, FE modeling, and an analysis of both posttraumatic scans and the anatomy of the bony orbital floor. Future studies should include more subjects and examine the biomechanics of materials used in reconstruction of the orbital floor.

ARTICLE INFORMATION

Accepted for Publication: December 6, 2016.

Published Online: March 9, 2017. doi:10.1001/jamafacial.2016.2153

Author Contributions: *Study concept and design:* Patel, Andrecovich, Zhang, Shkoukani. *Acquisition, analysis, or interpretation of data:* All authors. *Drafting of the manuscript:* Patel, Andrecovich, Silverman, Shkoukani. *Critical revision of the manuscript for important intellectual content:* Patel, Zhang, Shkoukani. *Statistical analysis:* Patel, Andrecovich, Shkoukani. *Obtained funding:* Patel, Shkoukani. *Administrative, technical, or material support:* Andrecovich, Silverman, Zhang, Shkoukani. *Supervision:* Patel, Zhang, Shkoukani.

Conflict of Interest Disclosures: None reported.

Funding/Support: Funding for the research was provided by the American Academy of Facial Plastic and Reconstructive Surgery (AAFPRS) Leslie Bernstein resident research grant.

Role of the Funder/Sponsor: We are grateful for the philanthropic gift from the AAFPRS. The funding source had no role in the design and conduct of the study; collection, management, analysis, and interpretation of the data; preparation, review, or approval of the manuscript; and decision to submit the manuscript for publication.

Additional Contributions: We thank Sanar Yokhana, MD, Department of Orthopedic Surgery, for his help with the cadaveric testing; Zhou Runzhou, MS, Department of Biomedical Engineering, for his help with the finite element analysis; and John Cavanaugh, MD, Department of Biomedical Engineering, and the late Robert H. Mathog, MD, Department of Otolaryngology, for their mentorship. They are all from Wayne State University and were not compensated for their assistance.

REFERENCES

1. Smith B, Regan WF Jr. Blow-out fracture of the orbit; mechanism and correction of internal orbital fracture. *Am J Ophthalmol*. 1957;44(6):733-739.

2. Tessier P. The classic reprint: experimental study of fractures of the upper jaw, I and II: René Le Fort, M.D. *Plast Reconstr Surg*. 1972;50(5):497-506.

3. Pfeiffer RL. Traumatic enophthalmos. *Trans Am Ophthalmol Soc*. 1943;41:293-306.

4. Raflo GT. Blow-in and blow-out fractures of the orbit: clinical correlations and proposed mechanisms. *Ophthalmic Surg*. 1984;15(2):114-119.

5. Jones DEP, Evans JNG. "Blow-out" fractures of the orbit: an investigation into their anatomical basis. *J Laryngol Otol*. 1967;81(10):1109-1120.

6. Phalen JJ, Baumel JJ, Kaplan PA. Orbital floor fractures: a reassessment of pathogenesis. *Nebr Med J*. 1990;75(5):100-103.

7. Ahmad F, Kirkpatrick WN, Lyne J, Urdang M, Garey LJ, Waterhouse N. Strain gauge biomechanical evaluation of forces in orbital floor fractures. *Br J Plast Surg*. 2003;56(1):3-9.

8. Zhang L, Yang KH, Dwarampudi R, et al. Recent advances in brain injury research: a new human head model development and validation. *Stapp Car Crash J*. 2001;45(45):369-394.

9. Zhang L, Sharma S. Development and Validation of A Detailed Finite Element Model of Human Eye for Predicting Ocular Trauma. Proceedings of Wayne State University; 75th Anniversary Symposium on Injury Biomechanics, Prevention, Diagnosis & Treatment; August 14-16, 2014. Detroit, Michigan.

10. Rhee JS, Kilde J, Yoganadan N, Pintar F. Orbital blowout fractures: experimental evidence for the pure hydraulic theory. *Arch Facial Plast Surg*. 2002;4(2):98-101.

11. Donat TL, Endress C, Mathog RH. Facial fracture classification according to skeletal support mechanisms. *Arch Otolaryngol Head Neck Surg*. 1998;124(12):1306-1314.

12. Cormier J, Manoogian S, Bisplinghoff J, et al. The tolerance of the frontal bone to blunt impact. *J Biomech Eng*. 2011;133(2):021004.